Atmos. Chem. Phys., 13, 4487–4500, 2013
www.atmos-chem-phys.net/13/4487/2013/
doi:10.5194/acp-13-4487-2013

Atmospheric Chemistry and Physics Open Access

Evaluation of a new middle-lower tropospheric CO_2 product using data assimilation

A. Tangborn[1], L. L. Strow[2], B. Imbiriba[3,*], L. Ott[4], and S. Pawson[4]

[1]Joint Center for Earth Systems Technology, University of Maryland Baltimore County, Baltimore, MD, USA
[2]Dept. of Physics, University of Maryland Baltimore County, Baltimore, MD, USA
[3]Núcleo de Meio Ambiente, Universidade Federal do Pará, Belém, PA, Brazil
[4]Global Modeling and Assimilation Office, Goddard Space Flight Center, Greenbelt, MD, USA
[*]currently at: Joint Center for Earth Systems Technology, University of Maryland Baltimore County, Baltimore, MD, USA

Correspondence to: A. Tangborn (tangborn@umbc.edu)

Received: 17 August 2012 – Published in Atmos. Chem. Phys. Discuss.: 10 October 2012
Revised: 5 April 2013 – Accepted: 11 April 2013 – Published: 2 May 2013

Abstract. Atmospheric CO_2 retrievals with peak sensitivity in the mid- to lower troposphere from the Atmospheric Infrared Sounder (AIRS) have been assimilated into the GEOS-5 (Goddard Earth Observing System Model, Version 5) constituent assimilation system for the period 1 January 2005 to 31 December 2006. A corresponding model simulation, using identical initial conditions, circulation, and CO_2 boundary fluxes was also completed. The analyzed and simulated CO_2 fields are compared with surface measurements globally and aircraft measurements over North America. Surface level monthly mean CO_2 values show a marked improvement due to the assimilation in the Southern Hemisphere, while less consistent improvements are seen in the Northern Hemisphere. Mean differences with aircraft observations are reduced at all levels, with the largest decrease occurring in the mid-troposphere. The difference standard deviations are reduced slightly at all levels over the ocean, and all levels except the surface layer over land. These initial experiments indicate that the used channels contain useful information on CO_2 in the middle to lower troposphere. However, the benefits of assimilating these data are reduced over the land surface, where concentrations are dominated by uncertain local fluxes and where the observation density is quite low. Away from these regions, the study demonstrates the power of the data assimilation technique for evaluating data that are not co-located, in that the improvements in mid-tropospheric CO_2 by the sparsely distributed partial-column retrievals are transported by the model to the fixed in situ surface observation locations in more remote areas.

1 Introduction

A new atmospheric CO_2 product (University of Maryland Baltimore County; UMBC AIRS CO_2) has been retrieved from the Atmospheric Infrared Sounder (AIRS) instrument on NASA's (Earth Observing System) EOS-Aqua satellite. This study uses the Goddard Earth Observing System, Version 5 (GEOS-5) atmospheric data assimilation system (DAS) to evaluate, in an integrated global sense, the quality of these retrievals using a variety of independent, in situ CO_2 measurements. The study also provides an assessment of how adequately this relatively sparse set of retrievals from AIRS, with at best several hundred observations per day, can be used to produce maps of the global CO_2 concentrations.

The UMBC AIRS CO_2 retrieval uses spectral radiance measurements from the emitted infrared wavelengths near 4.2 microns, leading to CO_2 partial columns that are weighted more strongly to the lower troposphere than retrievals from the 15-micron channels. These latter bands have been used in several other AIRS-based CO_2 retrievals, including the Jet Propulsion Laboratory (JPL) product (Chahine et al., 2008) and the European Centre for Medium-Range Weather Forecasts (ECMWF) product (Engelen et al., 2009), although the latter study included several channels at the shorter wavelengths. It also differs substantially from CO_2 products retrieved from the Greenhouse Gas Observing Satellite (GOSAT/Ibuki) satellite (e.g., Yokota et al., 2009) that are based on reflected solar radiance measurements near 2 microns.

The UMBC AIRS CO_2 retrievals are performed at observation locations chosen using a stringent quality control process that restricts data to cloud-free, uncontaminated scenes (Strow and Hannon, 2008). The sparseness of these data and their global distribution, often over oceans, precludes the use of vicarious calibration exercises in their evaluation. By transforming the partial columns derived from the time series of AIRS data to global atmospheric concentration maps, the DAS provides a framework for evaluating the retrievals using existing CO_2 observations. While this approach does not replace the need for targeted evaluation efforts, it does provide an alternate methodology that uses existing observation networks. In this case, the DAS provides the observation operators (and their adjoints) that map between the partial columns at the observation locations and atmospheric concentrations on a specified grid, and the transport computations that effectively interpolate from the AIRS observation locations to the sparse locations of the in situ observations. The observations used for evaluation are local CO_2 concentrations at the surface and on aircraft flight tracks.

An additional benefit of the DAS is that the resultant maps of CO_2 concentrations are valuable resources for helping to understand the spatial-temporal structure of regional CO_2 distributions and assessing their consistency with surface fluxes. This study includes a comparison of a model simulation with the assimilated CO_2 data. Apart from the data constraint in the assimilation, the two products are derived using an identical system (initial states, transport, and surface fluxes), so that differences between the model and the assimilation can be attributed to the innovations computed by the DAS. These differences are a central part of the evaluation, but they are also used to help evaluate the realism of the surface flux distributions applied in the system. This puts the atmospheric DAS used in this work in the context of inverse model studies, in which new estimates of surface fluxes are computed as a part of the optimization (e.g., Chevallier et al., 2009; Baker et al., 2010; Feng et al., 2011).

The rest of the paper is organized as follows: The AIRS 4 µm retrievals are described in Sect. 2, followed by some background on the model and assimilation system in Sect. 3; the assimilation results and verification with in situ data are presented in Sect. 4, and the discussion is given in Sect. 5.

2 The AIRS CO_2 retrievals used in this work

The Atmospheric Infrared Sounder on NASA's Aqua satellite measures infrared radiances in the wavelength range 3.7 to 15.4 microns with 2378 channels. Many channels are sensitive to CO_2, including several around 15 µm that have peak sensitivity between 150 and 400 hPa (Chahine et al., 2008). The sensitivity function, described in detail below, indicate the contribution of the retrieved value from each layer of the atmosphere. Examples of the 15 µm sensitivity function are shown in Fig. 1a. The peak sensitivity is generally higher

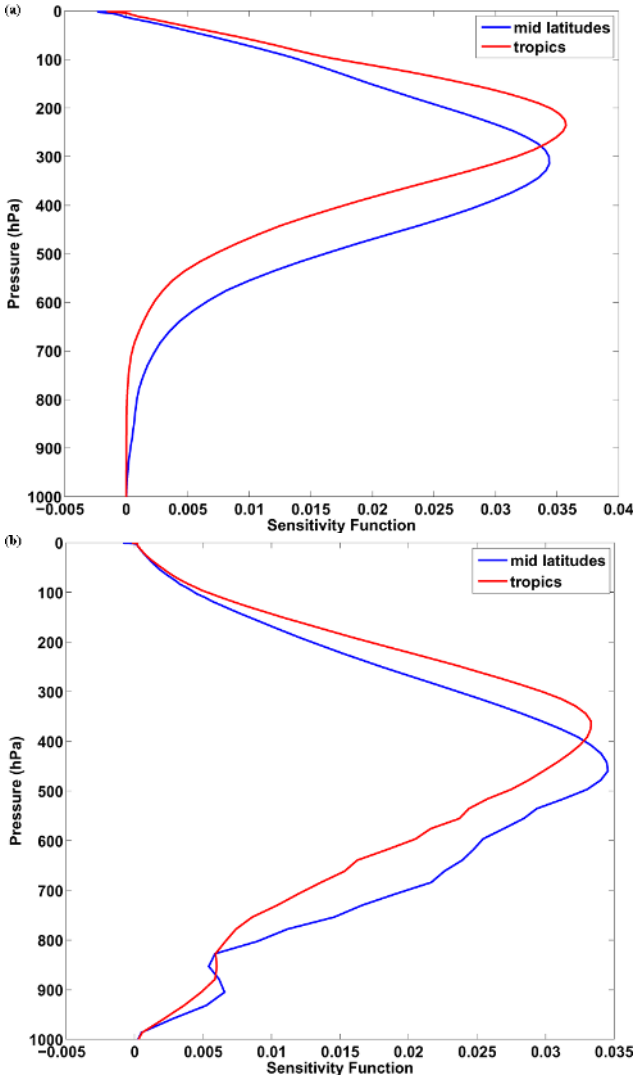

Fig. 1. Typical sensitivity functions for AIRS CO_2 retrieval from **(a)** a set of 15 µm spectral channels (e.g., Chahine et al., 2008), and **(b)** a cluster of channels near the 4 µm waveband.

in the tropics, and there is essentially no sensitivity below 700 mb. Given that one focus of atmospheric carbon cycle research is on improving estimates of surface fluxes, retrievals from channels with sensitivity lower in the troposphere are desirable.

In this work we use a cluster of channels in the 4 µm region (2400 cm^{-1}) that have peak sensitivity around 450 hPa. The actual channels used are 2388.87, 2389.84, 2390.82, 2391.80, 2415.56, 2416.56, 2417.56, and 2418.56 cm^{-1}. These channels have not been previously used in any CO_2 retrieval or assimilation. These channels were chosen for their sensitivity to CO_2 in the middle to lower troposphere, as shown by the sensitivity function in Fig. 1b. The eight channels make four pairs in which one channel is not sensitive to CO_2 and the other one is, which enables the CO_2 impacts

to be separated from atmospheric and surface effects on radiances. Using a cluster of channels reduces the statistical noise to 4.8 ppm per reported observation. The atmospheric state, including temperature profiles, is provided by the ECMWF analyses, which are interpolated in time and space to the precise AIRS observation event. In February 2006 there was a major change in the ECMWF system largely affecting the simulated temperature profiles and hence changing the bias in our retrieved CO_2 with respect to in situ measurements. In order to properly take this shift into account, the data needed to be recalibrated after this date. This one-time effect was treated with a single bias reduction of 2 ppm.

The retrievals used are restricted to clear sky observations only, which reduces the total observation count to a relatively small fraction of the AIRS measurements. In fact, there can be as many as four to five successive days in which there are no observations that pass through the cloud screening. The remaining observations are then superobbed to the model grid size ($2^\circ \times 2.5^\circ$) by taking a mean of all of the observations within the grid box. This reduces the representation error in the observations while ensuring that the matrix system (Eq. 5) is well conditioned. Figure 2 shows the observation counts for the superobbed data for the period January–February 2005. There are relatively few observations over continental regions, particularly North America and Asia, with a relatively greater number over oceans.

The retrievals are a least squares inversion for linear perturbations around the local ECMWF profile, which results in a mid–lower tropospheric CO_2 mixing ratio (see Rodgers, 2000). The inversion is done using the least squares inverse operator:

$$\mathbf{J}_{\mathrm{lsq}}^{-1} = \left[(\mathbf{J}^T \mathbf{J})^{-1} \mathbf{J}^T \right], \tag{1}$$

where the Jacobian, $\mathbf{J}$ is given by

$$\mathbf{J} = \left[\frac{\partial \boldsymbol{B}_{\mathrm{calc}}}{\partial T_{\mathrm{s}}}, \frac{\partial \boldsymbol{B}_{\mathrm{calc}}}{\partial \mathrm{CO}_2} \right], \tag{2}$$

where $\boldsymbol{B}_{\mathrm{calc}}$ is the vector of the brightness temperature calculated at the top of the atmosphere by applying the AIRS forward model to the EMCWF analysis fields. Additionally, T_{s} and CO_2 are the surface temperature and the carbon dioxide fields to be retrieved. The retrieval is then given by

$$[\delta T_{\mathrm{s}}, \delta \mathrm{CO}_2] = \sum_{\mathrm{c}} (mathbf J_{\mathrm{lsq}}^{-1})(\boldsymbol{B}_{\mathrm{o}} - \boldsymbol{B}_{\mathrm{calc}}), \tag{3}$$

where $[\delta T_{\mathrm{s}}, \delta \mathrm{CO}_2]$ and $(\boldsymbol{B}_{\mathrm{o}} - \boldsymbol{B}_{\mathrm{calc}})$ are the variations in the retrieved variables and bias brightness temperature (difference between observed and calculated brightness temperature), respectively.

The sensitivity function is obtained as a function of pressure level using the least squares inverse, applied to the variation of B_{calc} with respect to variations of CO_2 at pressure level i:

$$S_i^{\mathrm{CO}_2} = \sum_{\mathrm{c}} (J_{\mathrm{lsq}}^{-1})_{\mathrm{c}}^{\mathrm{CO}_2} \frac{\partial B_{\mathrm{c}}}{\partial \mathrm{CO}_2^i}, \tag{4}$$

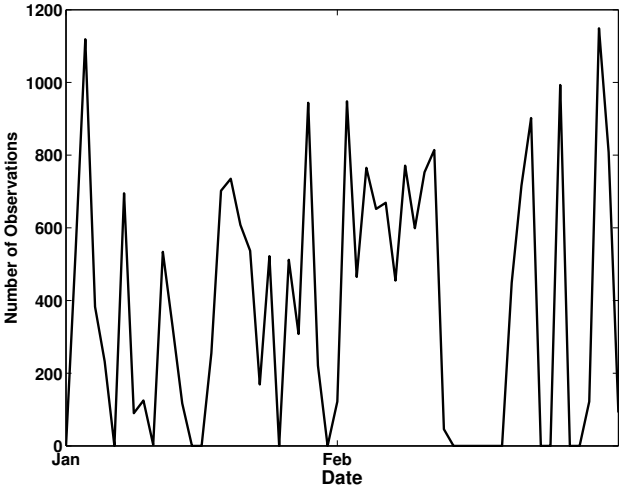

Fig. 2. Daily observation count for clear sky AIRS observations used in the data assimilation system for January–February 2005, superobbed to a $2^\circ \times 2.5^\circ$ grid.

where the subscript "c" refers to the spectral channels used. A typical sensitivity function (Fig. 1b) shows that the sensitivity at 700 hPa is still more than 1/3 of the peak level. The retrievals are validated with aircraft data and the differences are found to be on the order of 2 ppm. We use this number as the observation error standard deviation in the assimilation.

3 Transport model and assimilation system

The CO_2 assimilation module was originally developed for ozone (Stajner et al., 2001, 2008) and later adapted for CO (Tangborn et al., 2009). The algorithm is the Physical-space Statistical Analysis System (PSAS; Cohn et al., 1998), in which the standard 3DVAR (three-dimensional variation) is reformulated and solved in observation space. Thus the solution vector, solved by conjugate gradient methods, is the same length as the observation vector. This is a particularly efficient and attractive approach when assimilating relatively sparse observation sets, such as observations from a single satellite.

The current application of this system to AIRS CO_2 retrievals involves the introduction of the AIRS forward operator which consists of the following steps: interpolate the 72 model levels to the 101 sensitivity function pressure levels, $\mathbf{H}_{\mathrm{I}}$ (101×72 matrix); multiply the 101 CO_2 values by the appropriate sensitivity function, summing over all levels and divide by the sum of the sensitivity function values, $\mathbf{H}_{\mathrm{sf}}$ (1×101 matrix); thus the entire forward operator is $\mathbf{H} = \mathbf{H}_{\mathrm{sf}} \mathbf{H}_{\mathrm{I}}$. The PSAS algorithm solves the innovation equation

$$\left(\mathbf{H} \mathbf{P}^{\mathrm{f}} \mathbf{H}^T + \mathbf{R} \right) \boldsymbol{y} = \left(\boldsymbol{c}_{\mathrm{ca}}^{\mathrm{o}} - \mathcal{H}(\boldsymbol{x}^{\mathrm{f}}) \right) \tag{5}$$

for the vector $\boldsymbol{y}$, in observation space. Note that the length of $\boldsymbol{y}$ is equal to the number of observations. The linearization of the observation operator, $\mathcal{H}$, is $\mathbf{H}$, and error statistics are represented by the forecast error covariance, $\mathbf{P}^{\mathrm{f}}$. The observation error covariance, $\mathbf{R}$, is a diagonal matrix made up of observation error variances, which means that the observation errors are assumed to be spatially uncorrelated. The observations, c_{ca}, are column averaged using the sensitivity function with units of ppm.

The solution is then transformed to model space via

$$\boldsymbol{x}^{\mathrm{a}} - \boldsymbol{x}^{\mathrm{f}} = \mathbf{P}^{\mathrm{f}}\mathbf{H}^{T}\boldsymbol{y} \tag{6}$$

to obtain the analysis increment $\boldsymbol{x}^{\mathrm{a}} - \boldsymbol{x}^{\mathrm{f}}$, where $\boldsymbol{x}^{\mathrm{a}}$ is the CO_2 analysis and $\boldsymbol{x}^{\mathrm{f}}$ is the CO_2 forecast.

The forecast error covariance, $\mathbf{P}^{\mathrm{f}}$, is specified using a separable and non-isotropic error covariance model in which the error standard deviation, σ^{f}, is set as a constant percentage of the local CO_2 mixing ratio ($\sigma^{\mathrm{f}} = \alpha x^{\mathrm{f}}$) and the horizontal error correlation is a function of latitude. The correlation is an exponential function with a length scale of 100 km in the meridional direction, and the zonal length scale varies from 200 km in the tropics to 100 km in the high latitudes. Details of this correlation model are given in Stajner et al. (2001) and Tangborn et al. (2009). This results in a state-dependent error covariance because the error standard deviation is proportional to the CO_2 fields. Further adjustments to background errors are needed to account for the larger errors occurring in the Northern Hemisphere, which is discussed below. We have chosen to restrict corrections to the troposphere where CO_2 errors are generally larger than in the stratosphere. This is done by reducing the background error standard deviation in the stratosphere by a factor of 10.

Tuning runs were done in which the background standard deviation is varied using the standard deviation parameter α. Comparisons were then made with several ground- and aircraft-based in situ CO_2 data sets. These include measurements from the CCGG (Carbon Cycle Greenhouse Gases) Cooperative Air Sampling Network (Conway et al., 2011), NOAA GMD (Global Monitoring Division) Vertical Profile Carbon Cycle Network (aircraft data) and the Intercontinental Chemical Transport Experiment-Phase B (INTEX-B) (Singh et al., 2009). Initial testing showed that that a single value of α for the entire atmosphere is not sufficient because errors in the Northern Hemisphere are considerably higher than those in the Southern Hemisphere. This is even though the background-error model results in larger errors where CO_2 is higher, the comparisons with in situ data indicate that the error increase is even larger and tends to increase through the northern mid-latitudes. This increase is likely due to the larger variability (and therefore uncertainty) of CO_2 over continental land masses. Thus we use a factor α that depends on latitude. The optimal values of α from these tuning runs were found to be

$\alpha = 0.001$ for latitude $< 0°$,

$\alpha = 0.004$ for $0 \leq$ latitude $< 25°$ N,

$\alpha = 0.008$ for latitude $\geq 25°$ N.

These values of α result in surface background error standard deviations which vary from around 3 ppm in the northern mid-latitudes to about 0.35 ppm near the South Pole. This background model includes only latitudinal and geographic variations (since CO_2 is generally higher over land), but does not account for seasonal variation. For example, summer CO_2 values drop over North America, which would result in a drop in the estimated background errors using this model. However, we expect the uncertainty to remain high during this time because of uncertainty in the carbon uptake. Future versions of this assimilation system will include a seasonal correction using comparisons with in situ measurements, along with increased land errors to account for the uncertainty there.

This background error covariance model differs from previous AIRS CO_2 assimilation studies. Engelen et al. (2009) employed the NMC method (Parrish and Derber, 1992) which uses statistics from 24 and 48 h forecasts. This approach tends to underestimate errors where there are no observations, and they compensate for this by a factor of 8 inflation factor at the surface. But a constant inflation will not give the largest errors where flux estimate errors are the largest. Ensemble Kalman filter methodology shows great potential for estimating background errors (Liu et al., 2012), but this still does not address model errors as directly as comparison with in situ observations.

The CO_2 forecast fields, x^{f}, used by the assimilation are produced by the GEOS-5 Atmospheric General Circulation Model (AGCM), (Rienecker et al., 2008) using analyzed meteorology from the Modern-Era Retrospective Analysis for Research and Applications (MERRA; Rienecker et al., 2011). Biosphere and ocean CO_2 fluxes are prescribed based on the TRANSCOM (Atmospheric Tracer Transport Model Intercomparison Project)-3 protocol (Gurney et al., 2002). These fluxes assume a neutral biosphere meaning that the net flux over the course of a year is zero, while the ocean represents a 2.19 Gt C per year sink. Fossil fuel emissions representing the year 1998 are taken from the TRANSCOM-Continuous protocol (Law et al., 2008); the magnitude of the fossil fuel source is 6.58 Gt C per year. Biomass burning emissions follow the Global Fire Emissions Database version 2 (GFED-2; van der Werf et al., 2006). GFED-2 CO2 emissions were 2.34 Gt C for 2005 and 2.16 Gt C for 2006. This combination of fluxes likely results in a modestly high bias because of an underestimated carbon sink in TRANSCOM-3 and the fact that we are using biomass emissions not included in TRANSCOM. For this study, the model is run using a 2° latitude by 2.5° longitude horizontal resolution with 72 layers between the surface and 0.1 hPa.

4 Results

We have carried out a two year assimilation experiment for the period 1 January 2005 to 31 December 2006. A model simulation using identical initial states, meteorological fields and CO_2 boundary fluxes was also performed. Comparison of the assimilated and simulated CO_2 distributions allows the impact of the assimilation to be examined.

A typical analysis increment ($\boldsymbol{x}^{\mathrm{f}} - \boldsymbol{x}^{\mathrm{a}}$) at a latitude of 135° W is shown in Fig. 3. The rapid decay above 300 hPa is due to the reduced background errors in the stratosphere and the impact of the observation extends well into the lower troposphere. The shape of the increment depends on both the local sensitivity function and the local background error covariance.

Monthly mean CO_2 values at six CCGG surface flask sites are shown in Fig. 4, along with assimilated and simulated CO_2 fields, interpolated to the observation locations. These sites were chosen for their geographical distribution, and because they had at least 2 measurements per month over the assimilation period. Over the first few months, the assimilated (red curve) CO_2 diverges from the modeled (blue) fields, generally moving closer to the observations (black), indicating a spin-up time for the assimilation of about 6 months. This long period for the assimilation system to respond is most likely due to the small number of observations. In the Southern Hemisphere (panel a, b), where there is very little variation in CO_2, the improvements due to the assimilation are particularly significant because the initial difference between the model and observations is only about 1 ppm. At SPO (panel a), the initial high bias in the model becomes a modest low bias in the assimilation, indicating a possible low bias in the retrievals. However, the observations at SMO (panel b) result in a assimilation error well under 1 ppm.

In the northern mid-latitudes (panel c, d), the seasonal cycle is reproduced accurately in the model, but with a bias of 2–4 ppm. The assimilation reduces the bias, but does not significantly change the seasonal cycle. The flask site at 40° N (BAO) is the least successful, but still shows some reduction in the difference with measured values. Finally, in the northern high latitudes (panel f, g) the strong seasonal cycle is fairly well captured by the model. The assimilation reduces the bias, but it is not clear if there is a significant improvement to the annual cycle.

In order to get a more quantitative picture of how the assimilation is affecting the accuracy of the surface layer CO_2, we plot the mean and standard deviations of the difference between measurements and model or analyses (usually called observation minus model or analysis, O − M or O − A) at the six CCGG sites in Fig. 5. The mean differences (panel a) show a consistent decrease in the bias when the AIRS retrievals are assimilated. This decrease is particularly noteworthy in the Southern Hemisphere, where the declines are all more than 50 %. On the other hand, the standard deviation of the differences (panel b) show generally small

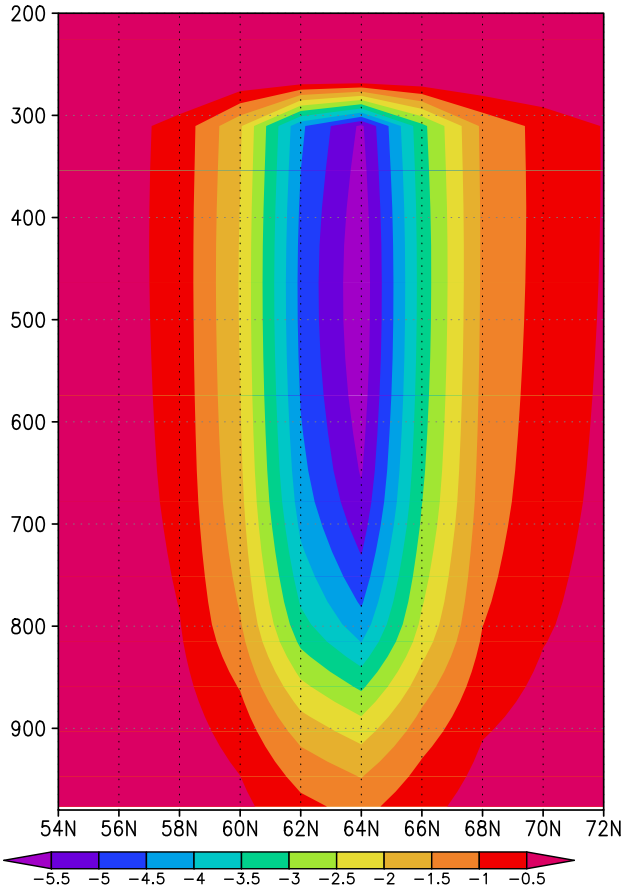

Fig. 3. The latitude-height structure of analysis increment for CO_2 (ppm) computed in GEOS-5 at 135° W, between 54° N and 72° N on 1 July 2006.

increases. This indicates that the assimilation is not helping to improve estimates of annual variability at these surface locations, in spite of the decrease in the bias. The lack of improvement in the random error at the surface most likely has two causes: the first is that this AIRS channel has peak sensitivity to CO_2 in the mid-troposphere, and essentially none inside the boundary layer. Thus any improvements that are made at the surface can only happen through corrections to CO_2 aloft that are transported to the surface by the model. We will discuss this process later in this section. The second cause is the sparsity of the clear sky AIRS observations. Figure 2 shows that there are many days when no observations are available, and sometimes none for several days at a time. This should impact the random error component to a greater degree because alternating between forcing the CO_2 field with observations and then allowing it to relax back towards the model state would likely add non-physical temporal variations into the field. Also, the long spin-up time for the assimilation (around 6 months) means that the assimilation cannot improve estimates for rapidly changing seasonal variations. This would be particularly true at the surface where

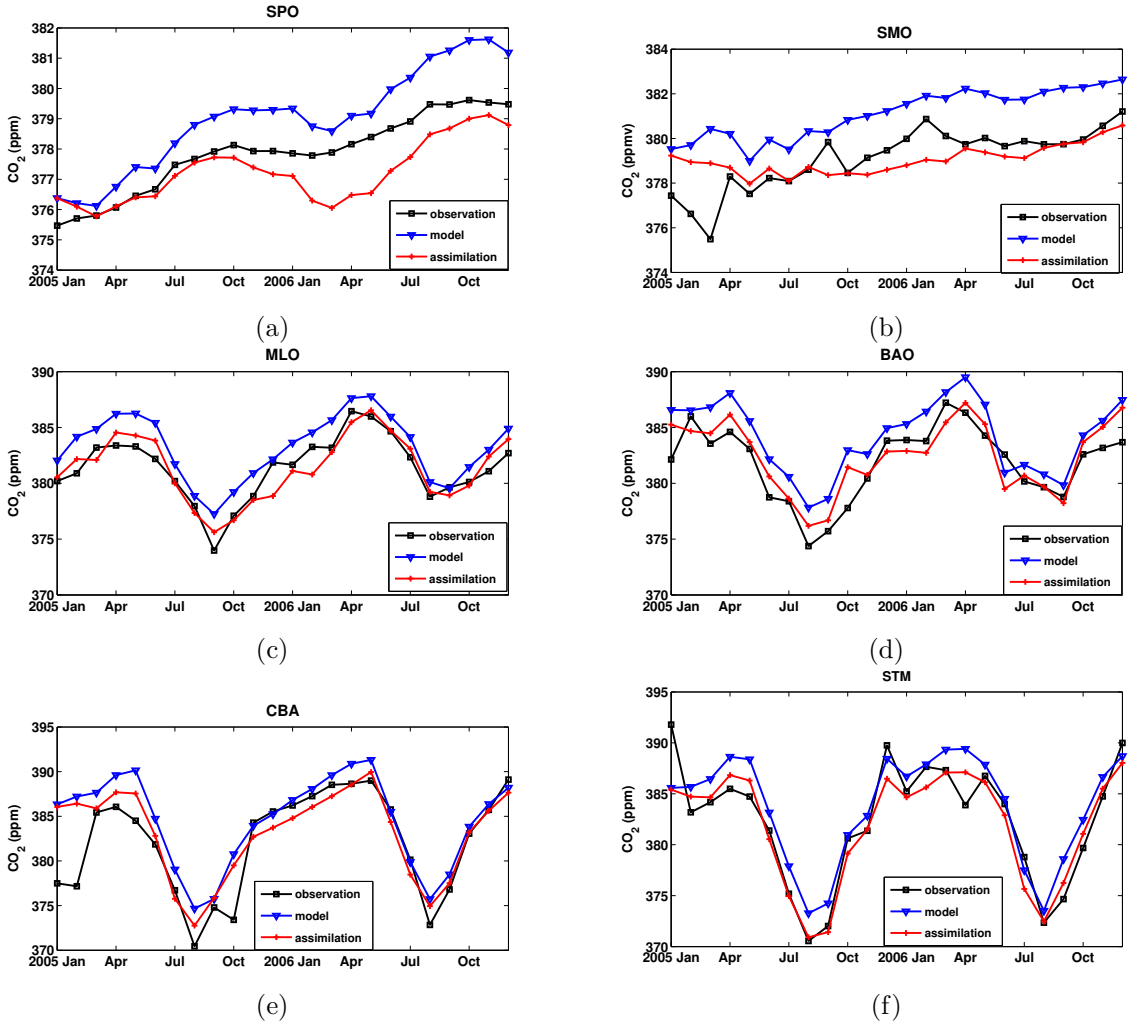

Fig. 4. Monthly mean CO_2 from NOAA/ESRL/GMD cooperative air sampling network (black), GEOS-5 interpolated to the observation locations, for simulations (blue) and with AIRS data assimilated (red). The sites used here are **(a)** SPO (89.96° S, 24.8° W), **(b)** SMO (14.25° S, 170.56° W), **(c)** MLO (19.5° N, 155.6° W), **(d)** BAO (40.0° N, 105.0° W), **(e)** CBA (55.2° N, 162.7° W), **(f)** STM (66° N, 2° E).

there is no direct impact of the observations. Mean and standard deviation differences between the model or assimilation and flask measurements for the entire set of measurements is shown in Fig. 6, separated into Northern and Southern hemispheres. These confirm that for all sites the mean differences drop significantly, while there is a smaller rise in the standard deviation.

There are a number of sources of in situ measurements from aircraft, and we have used two of these for assessing the impact of the assimilation. In Figs. 8 and 9 we plot the mean and standard deviation of the differences between the two model runs and NOAA/ESRL (Earth System Research Laboratory) aircraft data for 3 altitude ranges. Except for one exception (HAA, Hawaii), all of these measurements are made over continental North America where there are relatively few observations. The mean differences shows that the biggest improvements come in the mid-troposphere (panel b), while the surface (panel a) and upper troposphere (panel c) show somewhat mixed results, with slightly more than half the sites showing reduced differences with assimilation. This is consistent with the peak sensitivity of the retrieved AIRS channels at around 500 hPa. The standard deviations shown in Fig. 9 indicate very small changes due to the assimilation. At the surface (panel a), there are slightly more locations that show increases; while in the mid-troposphere (panel b), every location shows a modest decrease. In the upper troposphere (panel c), the very small changes are mainly downward.

The INTEX-B campaign carried out during February–May 2006, consisted of numerous flights across the central and western United States, as well as excursions over the Pacific Ocean (Fig. 7). So while there may be some overlap with the NOAA aircraft data, the main difference is that the flights are not done at discrete locations and involve travel over larger distances. In addition, the data available

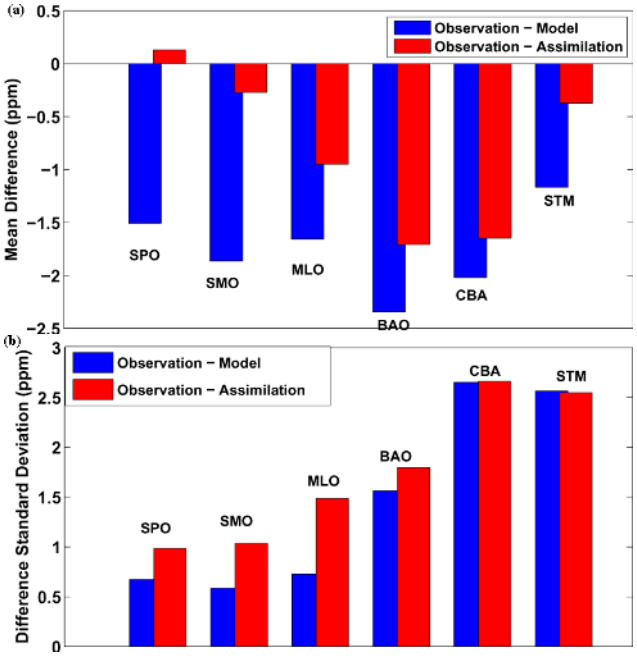

Fig. 5. Mean **(a)** and standard deviation **(b)** differences (O – M or O – A) between NOAA/ESRL/GMD cooperative air sampling network and model (blue) or analysis (red) fields interpolated to observation locations. The sites used here are the same as those in Fig. 4, and are ordered from south to north.

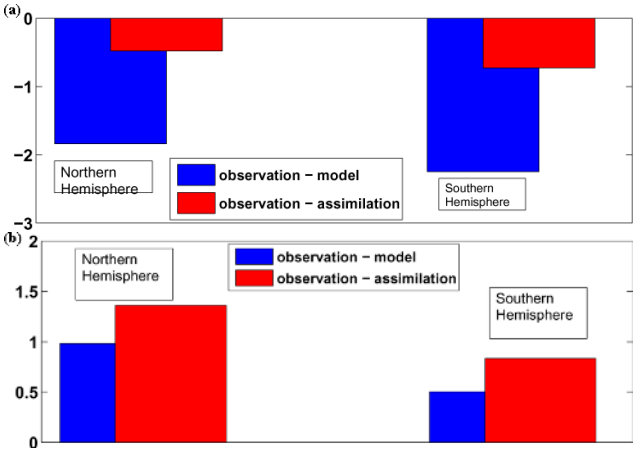

Fig. 6. Mean **(a)** and standard deviation **(b)** differences (O – M or O – A) between NOAA/ESRL/GMD cooperative air sampling network and model (blue) or analysis (red) fields interpolated to observation locations. These plots are for the entire set of measurements during the years 2005–2006.

for comparison is far greater due to the frequent sampling. We have divided the data into observations taken over the Pacific Ocean (panel a, b) and over North America (panel c, d), and mean and standard deviation differences (Forecast – Observation) in Fig. 10. Over the Pacific, the mean and standard deviation differences between the model and INTEX

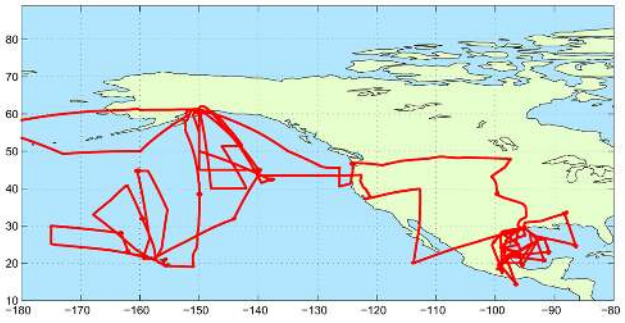

Fig. 7. Locations of measurements for INTEX-B flights, February–May 2006.

are smallest near the surface and increase with altitude, and they are reduced at all levels by the assimilation. This can be attributed to the small surface fluxes, which means that most of the CO_2 is transported over the ocean at higher levels. Over North America the differences are generally smaller at higher altitudes, particularly in the standard deviation, indicating that flux misspecification is the primary source of errors. While the mean differences are reduced by the assimilation at all levels, the standard deviation is only consistently reduced above 3000 m. The differences between the comparisons over the Pacific and North America are the result of larger fluxes (and therefore larger flux errors) and the smaller number of observations over land.

These results have some discrepancies with the NOAA aircraft comparisons. Most notable is that the magnitudes of both the mean and standard deviation differences over North America are smaller for INTEX-B than for NOAA aircraft data. This can be explained in part by the different regions of North America where data was collected, and probably is an indication that errors are not very uniform due to the higher variability. This can also been seen in the variability of the standard deviation differences with NOAA aircraft data, which range from 2 to 7 ppm. In order to make a more direct comparison, we have plotted the NOAA aircraft comparisons during the INTEX-B period (February–May 2006) for the middle troposphere (4000–5000 m) in Fig. 11. Note that some of the sites did not have sufficient measurements during this period to generate meaningful statistics, so they have been left out. The mean and standard deviation differences for this subset of aircraft data are generally larger than the full two year comparison, but still show the general trend of reduction in mean errors and relatively unchanged error standard deviations.

The improvement in the mean CO_2 fields at the surface that result from assimilating AIRS retrievals give some hope (but certainly does not guarantee) that these channels may be useful for CO_2 flux inversion, particularly when combined with other data sets. Baker et al. (2006) pointed out that in the tropics, model errors in vertical mixing tend to dominate, making it difficult to obtain an accurate estimate of

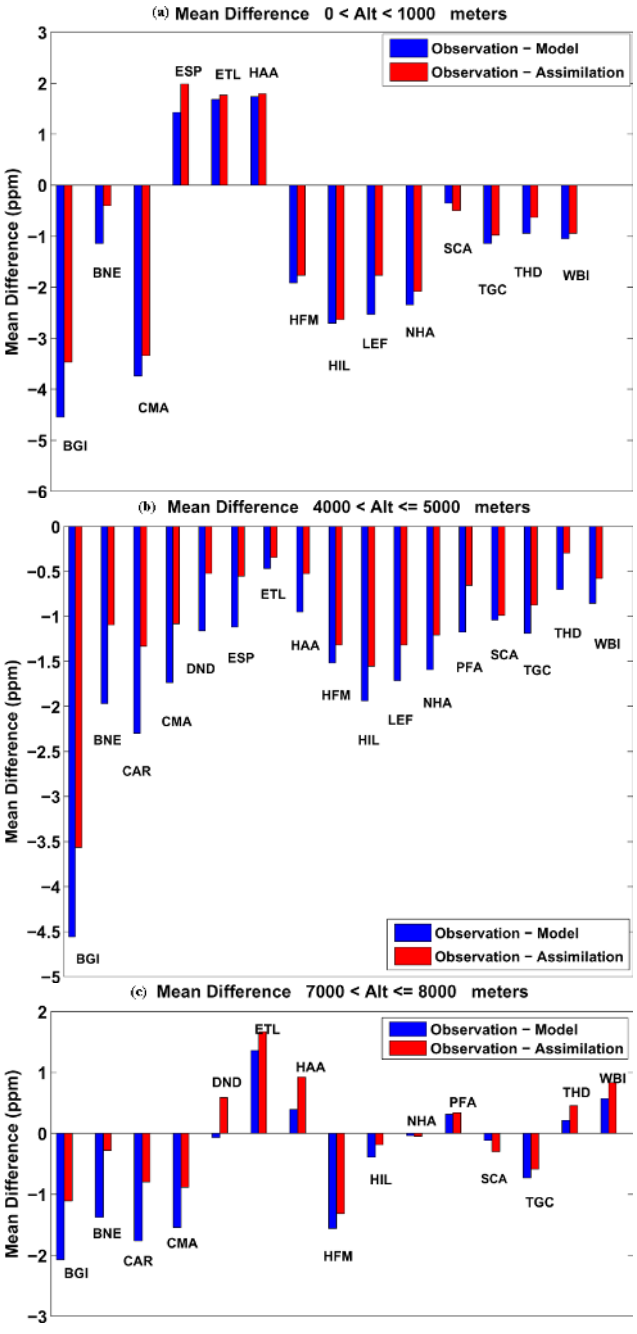

Fig. 8. Mean difference (Observation − Analysis) between the NOAA/ESRL aircraft data and CO_2 from the GEOS-5 model (or assimilation) interpolated to the observation locations, during the period 1 January 2005–31 December 2006.

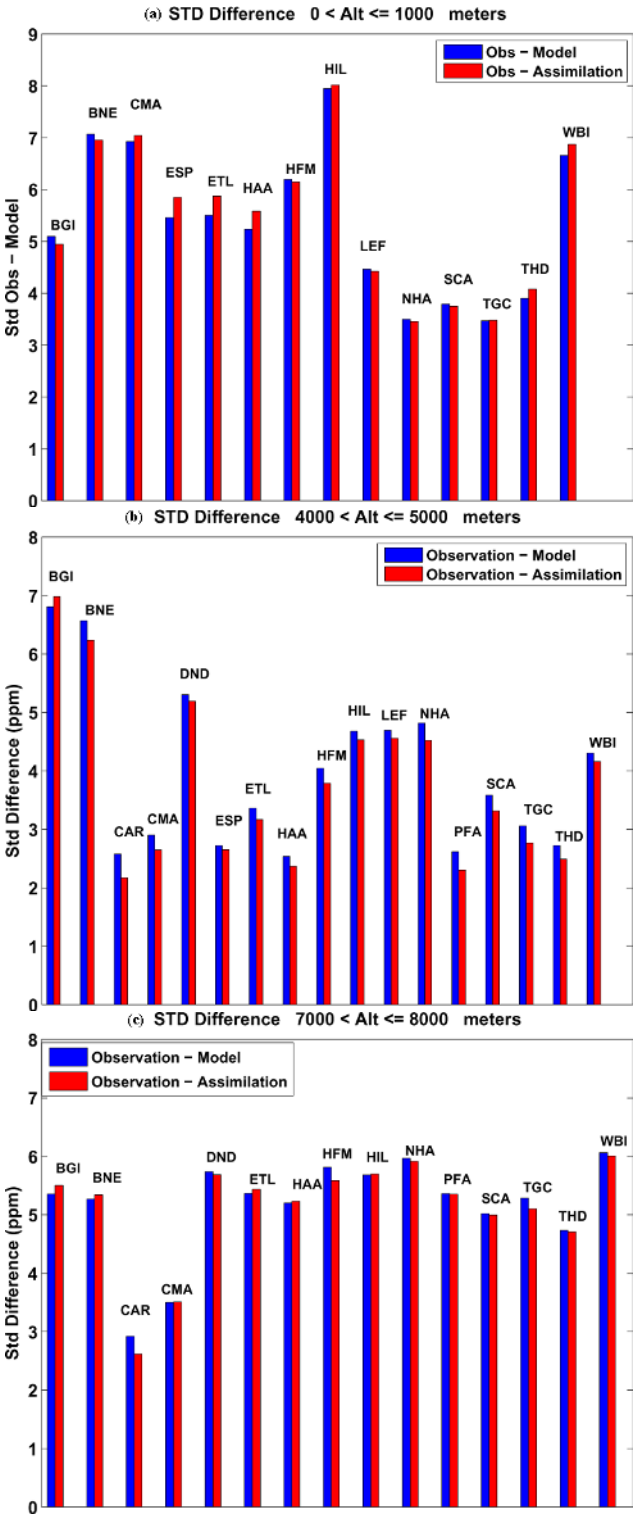

Fig. 9. Standard deviation of difference between the NOAA/ESRL aircraft data and CO_2 from the GEOS-5 model (or assimilation) interpolated to the observation locations, during the period 1 January 2005–31 December 2006.

CO_2 profiles. It would therefore be valuable to have additional tropospheric information of CO_2 with different vertical weightings. But the results above raise the questions as to how the assimilation of this data improves the mean comparisons in the surface layer, given that the peak sensitivity is around 500 hPa, with very little sensitivity at the surface. The most likely answer is that the assimilation makes corrections

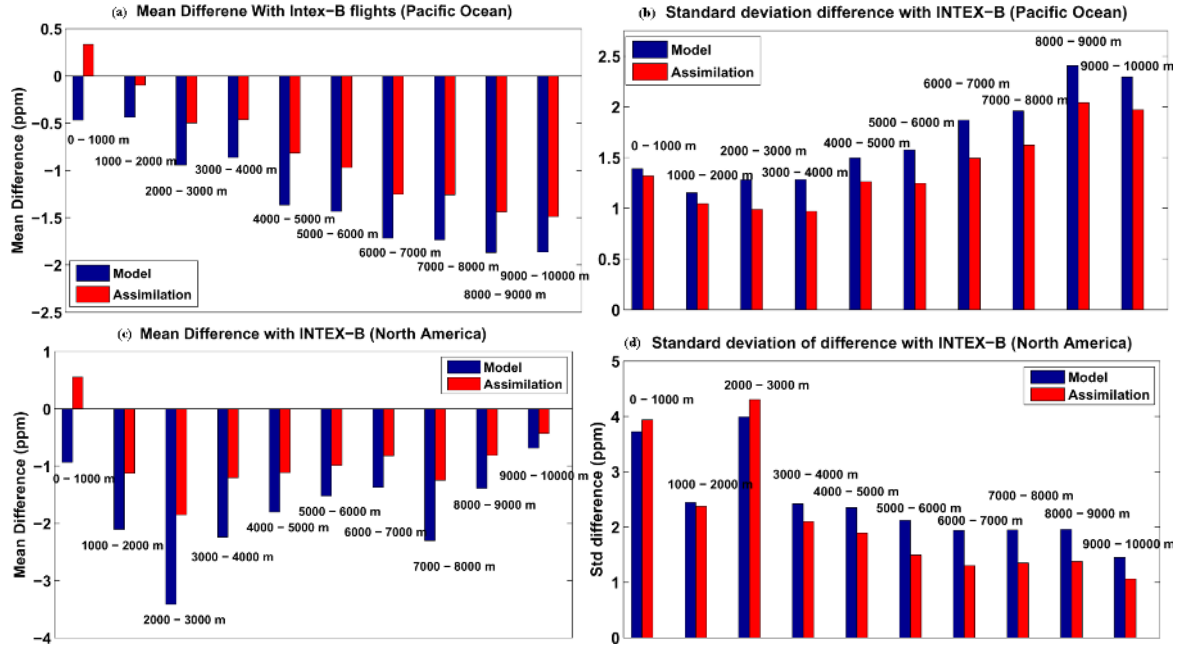

Fig. 10. Mean **(a)** and standard deviation **(b)** of difference (Observation − Analysis) between the INTEX-B campaign measurements and CO_2 from the GEOS-5 model (or assimilation) interpolated to observation locations over the Pacific Ocean, during the period February–May 2006. The same plots but with observations restricted to the flights over North America are shown in **(c)** and **(d)**.

centered in the 400 to 600 hPa range (about 4000 to 7000 m), which are then transported to the surface through convection in the model.

We investigate how improvements in mean CO_2 at the surface might take place by following the analysis increment from Fig. 3 during the first 24 h after assimilation. Figure 12 shows the difference between the assimilation run and the free model model run CO_2 in a vertical slice that follows the location of the maximum difference as it moves eastward. The difference between the two runs will consist of much more than one increment, and will also include differences from past observations. Nevertheless, this series of snapshots shows the clear evolution of a particular increment in the atmosphere (the data sparseness is an advantage for this analysis). In panel a, the initial negative difference can be seen near 64° N, 135° W, which is the result of an observation assimilated at 00:00 Z. The impact of the observation is maximum between 700 and 400 hPa. This structure is due to a combination of the sensitivity function, which peaks near 500 hPa, the background error variance (proportional to the local CO_2 mixing ratio), which is generally larger lower in the atmosphere, and the vertical error correlation. After 12 h (panel b), the peak difference has moved eastward and the difference at the surface has increased due to model transport. After 24 h (panel c), it is clear that though the increment is decaying (through atmospheric dispersion and mixing), it continues to have an impact at the surface as it moves eastward. These snapshots show how an observation in one region can impact the CO_2 field nearby, and how the mid-tropospheric

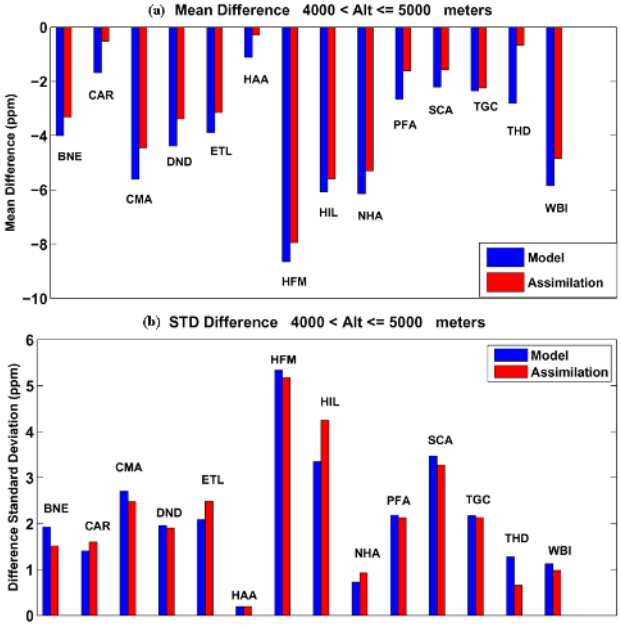

Fig. 11. Mean **(a)** and standard deviation **(b)** differences (O − M or O − A) between NOAA/CMDL aircraft measurements and model (blue) or analysis (red) fields interpolated to observation locations, for the period February–May 2006, and for measurements between 4000 to 5000 m. The sites used here are the same as those in Figs. 8 and 9, except for some which had too few measurements available during this period for calculating the standard deviation.

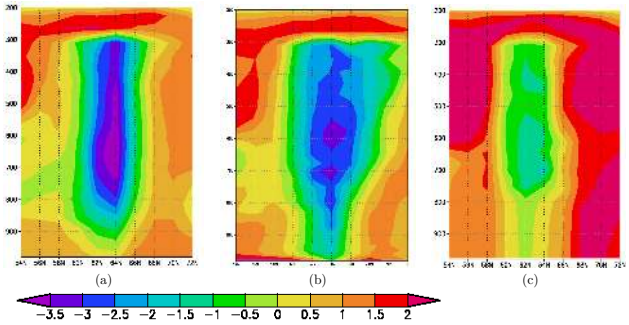

Fig. 12. Cross section of CO_2 differences between the assimilation and the simulation, along latitude lines that follow the local maximum difference on 1 July, 0Z, 135° W **(a)**; 1 July, 12Z, 130° W **(b)** and 2 July, 0Z, 125° W **(c)**.

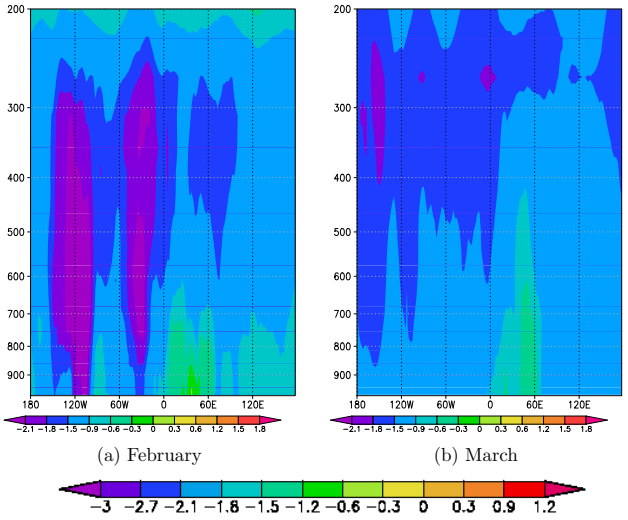

Fig. 13. Monthly mean differences between the assimilation run and free model run at 40° N, for February and March 2006.

sensitivity can translate into improvements at the surface. This is one possible explanation for the surface layer improvements shown in Fig. 4.

The contrast between the comparisons with NOAA/ESRL and INTEX-B aircraft measurements also needs further investigation. The mean differences between the assimilation and INTEX-B is between 0.5 and 1.0 ppm (even over North America), while the difference with NOAA/ESRL aircraft data varies from 0.5 to about 3.5 ppm. The disparity in the standard deviation differences is even more pronounced, 1 to 4 ppm compared with INTEX-B and 2 to 8 ppm compared with NOAA/ESRL. The INTEX-B measurements made over the eastern Pacific have lowest errors, while most of the NOAA/ESRL measurements are made over North America, where there are far fewer UMBC AIRS observations. These differences can be better understood by plotting monthly mean differences between the assimilation and free model run at 40° N, which is near many of the aircraft measurements. These differences, for the period February and March 2006 (the first 2 months of the INTEX-B campaign period), are shown in Fig. 13. Generally we see that the region over North America (about 120° W to 60° W) is changed much less than the adjacent ocean regions. For example, in February 2006 over the eastern Pacific and coastal North America (west of about 110° W), the largest changes the of CO_2 field reach down to the surface, while the change over most of North America are largest aloft.

We can use these comparisons to understand the mean and standard deviation differences with the NOAA/ESRL aircraft data. Figure 14 shows the NOAA/ESRL CO_2 profiles (black line) from Beaver Crossing, Nebraska, at (97° W, 40.8° N) along with the free model run (blue) and assimilation (red), interpolated to the profile locations. The profiles shown are monthly averages for February and March of 2006. In February, there is good coverage of AIRS CO_2 observations, and the analysis profile (Fig. 14a) is pulled towards the aircraft profile, but does not achieve the same vertical structure. During this time, Fig. 13a shows a large downward correction to CO_2 at all levels that reaches from the Pacific Ocean over western North America. During the first week of March, in contrast, there is a data gap in the AIRS data. And the result of this is that the CO_2 profile at BNE for this month is essentially the same for the assimilation and model. This results in assimilation profiles that have moved back towards the free running model profile during this month.

The temporal variations in the profile at BNE can also help to explain the error standard deviation differences with aircraft data. The analysis profile is seen to oscillate between the aircraft measurements (Fig. 14a), and the free running model profile (Fig. 14c). This type of movement causes an overall increase in the standard deviation difference with aircraft data, and is caused by the limited availability of retrievals over land. This contrasts with the consistently large decreases in error standard deviation differences with the INTEX-B aircraft data over the eastern Pacific for the assimilation, where a much larger number of retrievals are available.

Another way to analyze the impact of assimilation on the CO_2 fields is to calculate the total column (XCO_2) values both locally and regionally. In order to compare local XCO_2 against data collected from the Park Falls, Wisconsin Total Column Carbon Observing Network (TCCON) station (Wunch, et al., 2011), CO_2 profiles were extracted from GEOS-5 simulations at the grid cell containing Park Falls every 6 h. Individual TCCON observations were simulated by interpolating model CO_2 profiles to the time of the observation, and applying the sensitivity function appropriate for that observation's solar zenith angle to obtain a comparable, model-derived column CO_2 quantity. Daily means of TCCON observations and GEOS-5 results were then computed (Fig. 15) for the period January 2005–December 2006. The assimilation reduced the magnitude of the seasonal cycle slightly, and drew it closer to the measured values.

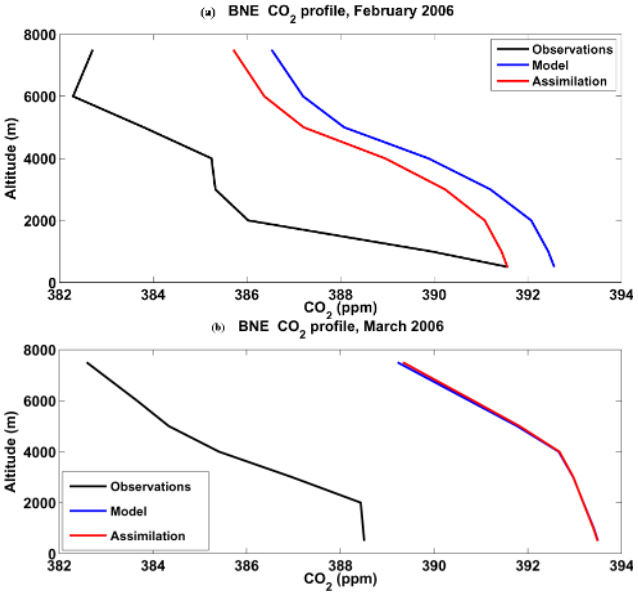

Fig. 14. Monthly mean profiles of CO_2 from CMDL aircraft data (black lines) at the Beaver Crossing, Nebraska (BNE, 97° W, 40.8° N), along with free running model (blue) and assimilation (red) output interpolated to the aircraft measurement locations, for February **(a)** and March **(b)** 2006.

Larger-scale changes in CO_2 due to the assimilation of AIRS retrievals can be examined by calculating the total column (XCO_2) over North America for both the free model and the assimilation runs. Figure 16 shows the comparison of the season cycle of column CO_2 over North America computed from January through December 2006, using the model and assimilation fields. The time series here has been detrended in order to capture only the annual cycle, so that any bias between the free model and assimilation run has been removed. The effect of the assimilation is to slightly reduce the magnitude of the seasonal cycle in column CO_2 from a 7.3 ppmv peak-to-trough amplitude in the model compared to a 6.4 ppmv amplitude when AIRS data are assimilated. The greatest differences occur in August and February–March. The changes to the seasonal cycle found here are probably smaller than would be obtained using a less sparse set of retrievals. It should be noted that these results include a single year of simulation; future work will consider a longer timer period to examine the impact of AIRS data over longer timescales.

5 Summary and discussion

A new atmospheric CO_2 partial-column data set, derived from a cluster of AIRS spectral radiance channels mainly near 4 µm, with peak sensitivity to CO_2 variations in the middle troposphere has been assimilated into GEOS-5. The stringent clear-sky criterion placed on these retrievals means that, at best, several hundred observations are available each day.

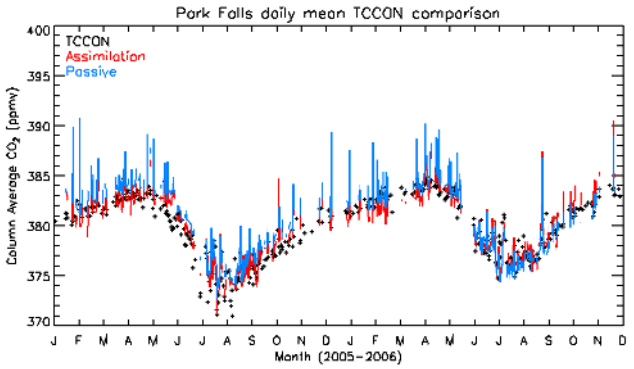

Fig. 15. Daily averaged total column CO_2 over Park Falls, Wisconsin for the period January to December 2006 for observations from TCCON (black), model (blue) and assimilation (red). The mean (bias) relative to TCCON is 1.2 ppm for the model, and 0.6 ppm for the assimilation. The RMS differences are 4.6 ppm for the model and 3.5 ppm for the assimilation.

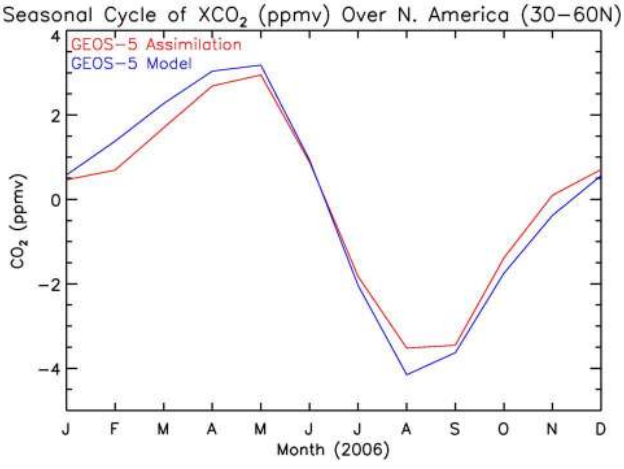

Fig. 16. Seasonal cycle of column-averaged CO_2 mixing ratio (ppmv) for the assimilation (red) and model (blue) calculated by detrending time series of monthly mean CO_2 over North America and then calculating departure from the annual (January through December 2006) mean.

The assimilation ran through 2005 and 2006. There are both positive and negative aspects of these results, which are discussed here.

One of the most positive aspects of this work is the generally beneficial impact of CO_2 data assimilation on the concentration distributions. The impacts of the assimilation are assessed using in situ measurements and comparing the assimilated distributions with those from an otherwise identical free-running model. Evaluation using surface flask observations reveals that, compared with the model simulation, the assimilation of the AIRS mid-tropospheric CO_2 retrievals improves the annual cycle in surface concentrations, especially in the Southern Hemisphere. Comparison with aircraft observations shows different impacts over land and oceans. Over North America, where NOAA aircraft observations are

routinely made, the assimilation leads to improvements in CO_2 near 500 hPa, with only a small benefit near the surface. Over the Pacific, comparison with aircraft observations from the INTEX-B field mission reveals larger positive impacts near the surface than over land. In the Southern Hemisphere and over oceans in the Northern Hemisphere, where local CO_2 fluxes are weak and where more observations are available to assimilate, the assimilation leads to substantial reductions in the mean bias compared to in situ observations. The standard deviation differences are not consistently reduced, but generally remain below 1 ppm in these regions.

This study does not propose that this sparse data set could be used alone to completely constrain the CO_2 field, or to be used as it is for flux inversion. The infrequent and relatively isolated analysis increments likely create non-physical spatial and temporal gradients that would make it difficult to use the data set for flux inversion. And even with a larger fraction of the measurements retrieved, the lack of vertical information in the observations precludes obtaining improved vertical gradients. But we have shown that there is significant information content in the observations, and that the information can be successfully spread to the surface layer to improve estimation of CO_2 there. This does imply that AIRS CO_2 from this particular set of channels should be included with future multisatellite assimilation efforts.

The CO_2 fluxes used in this work do contain bias as noted in Sect. 3. The mismatch between these imposed fluxes and the true ones (for the time and location of the assimilation) lead to atmospheric concentrations that depart substantially from the direct observations over North America. The strength of the fluxes, coupled with the absence of near-surface information content of these retrievals, means that the assimilation does not substantially improve the bias in CO_2 concentrations in this region. This means that more representative CO_2 fluxes need to be used in regions where they are large. However, regional maps of land biosphere CO_2 fluxes are known to have large uncertainties (e.g., Jung, et al., 2011), meaning that they result in large biases in the background state in the data assimilation system. Inverse approaches, that include the flux as a component of the state vector in the assimilation, offer the advantage of continuously correcting surface fluxes along with the atmospheric concentrations, but to date these also result in significant uncertainties (e.g., Baker et al., 2010; Feng et al., 2011; Nassar et al., 2011).

We cannot directly compare these results to other systems that have assimilated AIRS CO_2 since we are using a different set of fluxes and transport model. However, the in situ data sets used for validation in are generally the same, and some statement can be made in this respect. The work of Engelen et al. (2009) showed little improvement with respect to the NOAA/ESRL aircraft data, except in mean differences in the upper air CO_2 fields. Their mean model errors were of similar magnitude to those found in the present work, while the standard deviation differences were initially somewhat smaller. So the differences and the success of these different assimilation systems could be the result of model differences, or some differences in the data used.

There are also differences in error covariance modeling. The state dependent model used here accounts for variability due to the CO_2 field itself and is adjusted using comparisons with ground-based observations, whereas Engelen et al. (2009) used the NMC method, which tends to predict larger error growth where the observations are made. In a more recent work, Liu et al. (2012), assimilated CO_2 retrievals using channels near 15 μm and showed positive mean comparisons with in situ observations at all levels of the atmosphere. Much of this improvement can possibly be attributed to the use of the Local Transform Ensemble Kalman Filter (LETKF), which provides background error covariance estimates that reflect uncertainties in the meteorological fields. However, at some of the comparison locations, the free running model has a very large bias compared to the observations, so that improvements due to assimilation are relatively easy to achieve. It is likely that a hybrid approach that includes both ensemble error estimation and error statistics generated through comparisons with ground- and aircraft-based observations can account for errors that originate in both the transport and surface fluxes.

This system does not currently have in place a bias correction scheme, and the model (as with all CO_2 assimilation systems) does contain bias. Because the basic assumptions behind the PSAS algorithm is that both observations and forecasts are unbiased, the CO_2 analysis is necessarily less than optimal. The bias correction scheme used by Engelen et al. (2009) is the most appropriate approach to handle this issue. This involves the use of a regression model for the bias, and our plans are initially for the development of an off-line least-squares approach.

These results suggest that the UMBC AIRS CO_2 product is beneficial for constraining global atmospheric concentrations, despite the sparse spatial coverage. The version of the product used in this work was derived using meteorological fields from ECMWF, then assimilated into GEOS-5. A more robust long-term approach will investigate using GEOS-5 fields for all aspects of the work, including the possibility of cycling the retrievals through the assimilation system. This would allow use of GEOS-5 predictions of CO_2 as prior states in the retrieval, and also allow exploitation of consistent land-surface analyses that are being developed (e.g., Reichle et al., 2011).

Another aspect of this work that can be further exploited is the cross-calibration of different observations. For instance, extending the period of study to 2010–2011 will allow tests of the consistency between these NIR retrievals from AIRS with the reflected solar infrared measurements made by GOSAT (Yokota et al., 2009). Ultimately, the joint assimilation of CO_2 measurements from AIRS, GOSAT and other platforms is a highly desirable focus that should lead to better understanding of the atmospheric carbon balance.

Acknowledgements. The authors wish to thank Thomas Conway and Pieter Tans for the use of NOAA/ESRL CCG flask data, Colm Sweeney for the NOAA GMD Carbon Cycle Vertical Profile Network, and the INTEX-B team for access to this data set. TCCON data were obtained from the TCCON Data Archive, operated by the California Institute of Technology from the website at http://tccon.ipac.caltech.edu/. Computations were performed using the high-end computers at the NASA Center for Climate Simulation (NCCS). Comments from the 2 anonymous reviewers added greatly to the quality of this paper and are greatly appreciated.

Edited by: A. Geer

References

Baker, D. F., Law, R. M., Gurney, K. R., Rayner, P., Peylin, P., Denning, A. S., Bousquet, P., Bruhwiler, L., Chen, Y.-H., Ciasis, P., Fung, I. Y., Heimann, M., John, J., Maki, T., Maksyutov, S., Masarie, K., Prather, M., Pak, B., Taguchi, S., and Zhu, Z.: TransCom 3 inversion intercomparison: Impact of transport model errors on the interannual variability of regional CO_2 fluxes, 1988–2003, Global Biogeochem. Cy., 20, GB1002, doi:10.1029/2004GB002439, 2006.

Baker, D. F., Bösch, H., Doney, S. C., O'Brien, D., and Schimel, D. S.: Carbon source/sink information provided by column CO_2 measurements from the Orbiting Carbon Observatory, Atmos. Chem. Phys., 10, 4145–4165, doi:10.5194/acp-10-4145-2010, 2010.

Chahine, M. T., Chen, L., Dimotakis, P., Jian, X., Li, Q., Olsen, E. T., Pagano, T., Randerson, J., and Yung, Y. L.: Satellite remote sounding of mid-tropospheric CO_2, Geophys. Res. Lett., 35, L17807, doi:10.1029/2008GL035022, 2008.

Chevallier, F., Engelen, R. J., Carouge, C., Conway, T. J., Peylin, P., Pickett-Heaps, C., Ramonet, M., Rayner, P. J., and Xueref-Remy, I.: AIRS-based versus flask-based estimation of carbon surface fluxes, J. Geophys. Res., 114, D20303, doi:10.1029/2009JD012311, 2009.

Cohn, S. E., da Silva, A., Guo, J., Sienkiewicz, M., and Lamich, D.: Assessing the effects of data selection with the DAO physical-space statistical analysis system, Mon. Weather Rev., 126, 2913–2926, 1998.

Conway, T. J., Lang, P. M., and Masarie, K. A.: Atmospheric carbon dioxide dry air mole fractions from the NOAA ESRL Carbon Cycle Cooperative Global Air Sampling Network, 1968–2010, Version: 2011-10-14, available at: ftp://ftp.cmdl.noaa.gov/ccg/co2/flask/event/ (last access: September 2012), 2011.

Engelen, R. J., Serrar, S., and Chevallier, F.: Four-dimensional data assimilation of atmospheric CO_2 using AIRS observations, J. Geophys. Res., 114, D03303, doi:10.1029/2008JD010739, 2009.

Feng, L., Palmer, P. I., Yang, Y., Yantosca, R. M., Kawa, S. R., Paris, J.-D., Matsueda, H., and Machida, T.: Evaluating a 3-D transport model of atmospheric CO_2 using ground-based, aircraft, and space-borne data, Atmos. Chem. Phys., 11, 2789–2803, doi:10.5194/acp-11-2789-2011, 2011.

Gurney, K. R., Law, R. M., Denning, A. S., Rayner, P. J., Baker, D., Bousquet, P., Bruhwiler, L., Chen, Y. H., Ciais, P., Fan, S., Fung, I. Y., Gloor, M., Heimann, M., Higuchi, K., John, J., Maki, T., Maksyutov, S., Masarie, K., Peylin, P., Prather, M., Pak, B. C., Randerson, J., Sarmiento, J., Taguchi, S., Takahashi, T., and Yuen, C. W.: Towards robust regional estimates of CO_2 sources and sinks using atmospheric transport models, Nature, 415, 626–630, 2002.

Jung, M., Reichstein, M., Margolis, H. A., Cescatti, A., Richardson, A. D., Arain, M. A., Arneth, A., Bernhofer, C., Bonal, D., Chen, J. Q., Gianelle, D., Gobron, N., Kiely, G., Kutsch, W., Lasslop, G., Law, B. E., Lindroth, A., Merbold, L., Montagnani, L., Moors, E. J., Papale, D., Sottocornola, M., Vaccari, F., and Williams, C.: Global patterns of land-atmosphere fluxes of carbon dioxide, latent heat, and sensible heat derived from eddy covariance, satellite, and meteorological observations, J. Geophys. Res., 116, G00J07, doi:10.1029/2010JG001566, 2011.

Law, R. M., Peters, W., Rodenbeck, C., Aulagnier, C., Baker, I., Bergmann, D. J., Bousquet, P., Brandt, J., Bruhwiler, L., Cameron-Smith, P. J., Christensen, J. H., Delage, F., Denning, A. S., Fan, S., Geels, C., Houweling, S., Imasu, R., Karstens, U., Kawa, S. R., Kleist, J., Krol, M. C., Lin, S. J., Lokupitiya, R., Maki, T., Maksyutov, S., Niwa, Y., Onishi, R., Parazoo, N., Patra, P. K., Pieterse, G., Rivier, L., Satoh, M., Serrar, S., Taguchi, S., Takigawa, M., Vautard, R., Vermeulen, A. T., and Zhu, Z.: TransCom model simulations of hourly atmospheric CO_2: Experimental overview and diurnal cycle results for 2002, Global Biogeochem. Cy., 22, GB3009, doi:10.1029/2007GB003050, 2008.

Liu, J., Fung, I., Kalnay, E., Kang, J. S., Olsen, E. T., and Chen, L.: Simultaneous assimilation of AIRS XCO_2 and meteorological observations in a carbon climate model with an ensemble Kalman filter, J. Geophys. Res., 117, D05309, doi:10.1029/2011JD016642, 2012.

Nassar, R., Jones, D. B. A., Kulawik, S. S., Worden, J. R., Bowman, K. W., Andres, R. J., Suntharalingam, P., Chen, J. M., Brenninkmeijer, C. A. M., Schuck, T. J., Conway, T. J., and Worthy, D. E.: Inverse modeling of CO_2 sources and sinks using satellite observations of CO_2 from TES and surface flask measurements, Atmos. Chem. Phys., 11, 6029–6047, doi:10.5194/acp-11-6029-2011, 2011.

Parrish, D. F. and Derber, J. C.: The National Meteorological Center's spectral statistical-interpolation analysis system, Month. Weather Rev., 120, 1747–1763, 1992.

Rienecker, M. M., Suarez, M. J., Todling, R., Bacmeister, J., Takacs, L., Liu, H.-C., Gu, W., Sienkiewicz, M., Koster, R. D., Gelaro, R., Stajner, I., and Nielsen, J. E.: The GEOS-5 Data Assimilation System-Documentation of versions 5.0.1, 5.1.0, and 5.2.0, NASA Tech. Rep. 104606 V27, 2008.

Rienecker, M. M., Suarez, M. J., Gelaro, R., Todling, R., Bacmeister, J., Liu, E., Bosilovich, M. G., Schubert, S. D., Takacs, L., Kim, G. K., Bloom, S., Chen, J. Y., Collins, D., Conaty, A., Da Silva, A., Gu, W., Joiner, J., Koster, R. D., Lucchesi, R., Molod, A., Owens, T., Pawson, S., Pegion, P., Redder, C. R., Reichle, R., Robertson, F. R., Ruddick, A. G., Sienkiewicz, M., and Woollen, J.: MERRA – NASA's Modern-Era Retrospective Analysis for Research and Applications, J. Climate, 24, 3624–3648, 2011.

Reichle, R. H., Koster, R. D., De Lannoy, G. J. M., Forman, B. A., Liu, Q., Manhanama, S. P. P., and Toure, A.: Assessment and Enhancement of MERRA Land Surface Hydrology Estimates, J. Climate, 24, 6322–6338, doi:10.1175/JCLI-D-10-05033.1, 2011.

Rodgers, C. D.: Inverse Methods for Atmospheric Sounding, Theory and Practice, World Scientfic, Singapore, 2000.

Singh, H. B., Brune, W. H., Crawford, J. H., Flocke, F., and Jacob, D. J.: Chemistry and transport of pollution over the Gulf of Mexico and the Pacific: spring 2006 INTEX-B campaign overview and first results, Atmos. Chem. Phys., 9, 2301–2318, doi:10.5194/acp-9-2301-2009, 2009.

Stajner, I., Riishöjgaard, L. P., and Rood, R.B.: The GEOS ozone data assimilation system: Specification of error statistics, Q. J. Roy. Meteorol. Soc., 127, 1069–1094, 2001.

Stajner, I., Wargan, K., Pawson, S., Hayashi, H., Chang, L. P., Hudman, R. C., Froidevaux, L., Livesey, N., Levelt, P. F., Thompson, A. M., Tarasick, D. W., Stubi, R., Andersen, S. B., Yela, M., Konig-Langlo, G., Schmidlin, F. J., and Witte, J. C.: Assimilated Ozone from EOS-Aura: Evaluation of the Tropopause Region and Tropospheric Columns, J. Geophys. Res., 113, D16532, doi:10.1029/2007JD008863, 2008.

Strow, L. L. and Hannon, S. E.: A 4-year zonal climatology of lower tropospheric CO_2 derived from ocean-only Atmospheric Infrared Sounder observations, J. Geophys. Res., 113, D18302, doi:10.1029/2007JD009713, 2008.

Tangborn, A., Stajner, I., Buchwitz, M., Khlystova, I., Pawson, S., Hudman, R., and Nedelec, P.: Assimilation of SCIAMACHY total column CO observations; Global and regional analysis of data impact, J. Geophys. Res., 114, D07307, doi:10.1029/2008JD010781, 2009.

van der Werf, G. R., Randerson, J. T., Giglio, L., Collatz, G. J., Kasibhatla, P. S., and Arellano Jr., A. F.: Interannual variability in global biomass burning emissions from 1997 to 2004, Atmos. Chem. Phys., 6, 3423–3441, doi:10.5194/acp-6-3423-2006, 2006.

Wunch, D., Toon, G. C., Blavier, J.-F. L., Washenfelder, R. A., Notholt, J., Connor, B. J., Griffith, D. W. T., Sherlock, V., Wennberg, P. O.: The Total Carbon Column Observing Network, Phil. Trans. R. Soc. A, 369, 2087–2112, doi:10.1098/rsta.2010.0240, 2011.

Yokota, T., Yoshida, Y., Eguchi, N., Ota, Y., Tanaka, T., Watanabe, H., and Maksyutov, S.: Global Concentrations of CO_2 and CH_4 Retrieved from GOSsAT: First Preliminary Results, SOLA, 5, 160–163, doi:10.2151/sola.2009-041, 2009.